Aquaculture International (2024) 32:5415–5435
https://doi.org/10.1007/s10499-024-01430-6

Ran in *Procambarus clarkii*: molecular characterization and immune function

Yanlong Gu[1] · Tong Zhao[1] · Xinru Wang[1] · Libo Hou[1] · Hao Li[1] · Lei Zhu[1] · Xianghui Kong[1]

Received: 9 January 2024 / Accepted: 7 February 2024 / Published online: 14 February 2024

Abstract
As a member of the small G protein superfamily, ras-related nuclear proteins (Ran) mainly function in regulating nucleocytoplasmic transport and microtubule formation. Ran is reported to have an immune function in invertebrate defense against pathogen invasion. This study obtained the full-length sequence of the *Ran* cDNA (*PcRan*) of *Procambarus clarkii* and investigated changes in its expression after pathogenic infection and its role in the clearance of pathogenic bacteria. Phylogenetic tree analysis revealed that PcRan and Ran of other crustaceans belong to one branch and have a close genetic relationship. Multiple sequence alignment analyses revealed that PcRan has a highly conserved G domain and contains all the G1–G5 motifs. *PcRan* expression was widely distributed in various tissues in *P. clarkii*, with the highest expression levels being found in the muscle and gills. The levels of *PcRan* expression in several major immune organs, including hepatopancreas, gills, hemocytes, and intestines, were significantly increased after infection with white spot syndrome virus or *Aeromonas veronii*. After *PcRan* overexpression, the bacterial clearance ability and survival rate of *P. clarkii* infected with *A. veronii* was significantly higher than that of the control group. This study showed that PcRan is involved in the innate immune process of *P. clarkii*. The results of this study provide theoretical significance and application value for understanding the immune function of Ran after crayfish pathogen infection, and provide guidance for the prevention and control of crayfish diseases.

Keywords *Procambarus clarkii* · *Ran* · Molecular characterization · Immune function · *Aeromonas veronii*

Handling Editor: Brian Austin

✉ Lei Zhu
zhulei@htu.edu.cn

[1] Engineering Lab of Henan Province for Aquatic Animal Disease Control, College of Fisheries, Henan Normal University, Xinxiang 453007, China

Introduction

Ras-related nuclear protein (Ran) is a member of the small G protein superfamily. In 1990, Drivas et al. (1990) first discovered the open reading frame (ORF) of Ran in the cDNA of human teratoma cells. Bischoff and Ponstingl (1991) isolated Ran from HeLa cells. The Ran polypeptide molecule that forms a complex with RCC1, the mitosis inhibitory regulatory protein (later demonstrated to be the guanylate exchange factor of Ran) in cells, is the most abundant small G protein.

Ran exhibits GTPase activity, can connect and hydrolyze GTP, and is an important regulator of many metabolic pathways. Ran is involved in several biological processes in eukaryotic cells, such as DNA replication, RNA transcription and processing (or modification), and nucleo-cytoplasmic transportation (Seki et al. 1992; Ach and Gruissem 1994; Sazer 1996; Mattaj and Englmeier 1998; Clarke and Zhang 2001; Moore 2001). The Ran protein is highly conserved (Hetzer et al. 2002). The highly conserved G domain of the Ran protein consists of five motifs (G boxes): G1 (GXXXXGK[S/T], G2 (XTX), G3 (DXXG), G4 (N/T) (K/Q)XD, and G5 [(T/G/C) (C/S) AK)] (where X is any amino acid) (Yang 2002; Toma-Fukai and Shimizu 2019).

Because of the important role of *Ran*, it has attracted widespread research attention. In fishes, *Ran* has been identified in *Salmo salar* (Lundin et al. 2000), *Carassius auratus* color variety (Li et al. 2003), and *Carassius auratus gibelio* (Li et al. 2006). In *Penaeus japonicus*, an important function of Ran GTPase is to regulate hemocytic phagocytosis by interacting with myosin, β-actin, and Ran. Research have also reported that in shrimp, Ran GTPases play a new role in immunity against pathogenic infections. *Pj*Ran interacts with myosin to regulate phagocytosis of shrimp hemocytes (Liu et al. 2009). The mRNA level of *Ran* significantly changed in virus-infected shrimp suggesting *Ran* plays an important role in the host response to viral infection (Han and Zhang 2007). Ning et al. (2017) cloned and identified *Ran* in *Macrobrachium rosenbergii*; over-expression of *MrRan* enhanced phagocytosis in response to *Spiroplasma eriocheiris* challenge in *M. rosenbergii*. These data suggested that Ran may play an important role in the host immune response to pathogen infection.

As a lower invertebrate, red swamp crayfish (*Procambarus clarkii*) mainly relies on innate immunity to resist the invasion of pathogens (Wan et al. 2022). With the intensive farming of crayfish and the degradation of germplasm resources, the crayfish farming industry is threatened by serious diseases, affecting its viability. Among them, infections by *Aeromonas veronii* and white spot syndrome virus (WSSV) are the main diseases that affect the growth and sustainability of crayfish farming (Gu et al. 2023). Therefore, to prevent disease, in-depth analysis of the immune defense mechanism of crayfish is considered to be the most fundamental and effective method (Fu et al. 2023).

Although various studies related to the Ran protein have been conducted, the role and mechanism of the Ran protein in the immune function of crayfish are not fully understood. In our study, we aimed to explore the molecular characteristics of *PcRan* and its immune response characteristics in response to *A. veronii* infection, along with its role in immune response during pathogenic infection. It is believed that this study can provide a theoretical basis for the immune function of *Ran* of *P. clarkii* and can also provide theoretical support for the prevention and control of crustacean diseases.

Materials and methods

Experimental red swamp crayfish and feeding methods

Healthy crayfish (weighing 25–30 g) were collected from Huai'an, Jiangsu, China. *Procambarus clarkii* was acclimatized by growing in a rectangular tank (with continuous aeration and UV-treated freshwater; pH, 7.5–8.5; transparency, 20–25 cm; dissolved oxygen, > 2 mg/L; water temperature, 25 ± 0.5 °C) in a laboratory for 1 week. During the acclimation period, crayfish were fed commercial feed (Tongwei Co., Ltd., China) twice daily until feeding was stopped 3 d before the experiment. All animal experiments in this study were approved (Approval no: HNSD-2024-BS-0130) by the Institutional Laboratory Animal Care and Use Committee of Henan Normal University.

RNA extraction and cDNA synthesis

Gills were extracted from five healthy crayfish under sterile conditions. RNA was extracted with the Total RNA Extraction Reagent (Vazyme, Nanjing, China) following the manufacturer's protocol. RNA purity was verified using a NanoDrop 2000 spectrophotometer (Thermo Scientific, Inc., USA), and RNA integrity was assessed using agarose gel electrophoresis.

A PrimeScript™ II 1st strand cDNA Synthesis kit (TaKaRa, Japan) was used to synthesize first-strand cDNA for gene cloning. The reaction system included 4 μL of total RNA, 2 μL of Oligo dT primer, 2 μL of dNTP mixture, and 12 μL of RNase-free ddH_2O. The mixture was reacted in a polymerase chain reaction (PCR) machine at 62 °C for 5 min. Subsequently, the RNA was reverse transcribed into the cDNA template according to the manufacturer's instructions. The cDNA was stored at − 20 °C until use.

cDNA cloning of PcRan

Based on the predicted sequence of *PcRan* in the NCBI database (XM_045758666.1), using *P. clarkii* gills as the cDNA template, *PcRan*-specific primers were designed with the help of Primer 5.0 to amplify its ORF sequence. The PCR mix of 25 μL contained 12.5 μL of 2 × Taq Plus Master Mix, 1 μL of each primer, 1 μL cDNA template, and 9.5 μL of ddH_2O. The PCR protocol was as follows: pre-denaturation at 95 °C for 5 min; 34 cycles of 95 °C for 30 s, 60 °C for 30 s, and 72 °C for 2 min; and a final extension at 72 °C for 10 min. The PCR product was purified and cloned into the pMD19-T plasmid (TaKaRa, Japan). The plasmids were used to transform DH5α chemically competent cells (TaKaRa, Japan), and single colonies of positive clones were selected for sequencing. From these, *PcRan* was sequenced by GENEWIZ Biotech (Suzhou, China).

To obtain the full-length sequence of *PcRan*, 5′ and 3′ cDNA sequences were synthesized for rapid amplification of cDNA ends (RACE). For 3′ RACE template preparation, the PrimeScript™ II First Strand cDNA Synthesis Kit instructions were followed as described in the "RNA extraction and cDNA synthesis" section, replacing the Oligo dT Primer with the 3′ RACE Olig(T)-adaptor for reverse transcription. For the 5′ RACE amplification template, the obtained cDNA product was purified using E.Z.N.A.™ Cycle-pure Kit (Omega, USA), and a poly(A) tail was added to the 3′ end of the purified product. The total reaction volume of 50 μL contained 10 μL of cDNA, 5 μL of 1% Bovine Serum Albumin (BSA), 10 μL of 5 × terminal deoxynucleotidyl transferase (TdT) buffer, 1

μL of TdT enzyme, 2.5 μL of dATP, and 21.5 μL of ddH_2O. The reaction conditions were 37 °C for 30 min and 80 °C for 3 min. The first round of PCR amplification was performed using primers *Ran 3′-Out*/*Ran 5′-Out* and *3′ RACE Adapter*/*5′ RACE Olig(T)-Adaptor*. The PCR product obtained from the first round was diluted 50 times and used as the PCR template in the second round. The second round of amplification was performed using nested PCR using the primers *Ran 3′-In*/*Ran 5′-In* and *3′ RACE Adapter*/*5′ RACE Adapter*. The reaction procedure was the same as the ORF amplification procedure described in the "RNA extraction and cDNA synthesis" section, except that the number of first-round PCR cycles was reduced to 20 (Zhao et al. 2023a). The primer sequences used are listed in Table 1. The three amplified cDNA sequences were spliced using DNAMAN software to obtain the full-length sequence of *PcRan*.

Bioinformatic analyses

Homology analysis of the cDNA sequence of *PcRan* was performed using the BLAST program (http://blast.ncbi. nlm.nih.gov/Blast.cgi). The protein domain of PcRan was predicted using the SMART program (http://smart.embl-heidelberg.de/). The online software SWISS-MODEL (https://swissmodel.expasy.org/) was used to predict the three-dimensional structure of PcRan. The Compute pI/Mw module (http://web.expasy.org/compute_pi/) was used to calculate the molecular weight and theoretical isoelectric point of the PcRan protein. The phylogenetic tree was constructed by the neighbor-joining method using MEGA 8.0 software (Kumar et al. 2016) and its reliability was verified using 1000 bootstraps.

Tissue distribution of PcRan

Different tissues (gills, hemocytes, intestine, hepatopancreas, heart, stomach, muscle, and gonads) were collected from five healthy crayfish. The specific primers *Ran-F2* and *Ran-R2* were used to detect the expression levels of *PcRan* mRNA in these different tissues, and *18S* RNA (see Table 1 for primer sequences) was used as the internal reference gene (Qin et al. 2019). The SYBR Premix Ex Taq™ II kit (TaKaRa, Japan) was used to conduct the quantitative real-time PCR (qRT-PCR), following the manufacturer's protocols. The qRT-PCR steps were as follows: preincubation at 95 °C for 30 s followed by 40 cycles of 95 °C for 15 s, 60 °C for 10 s, and 72 °C for 20 s. To ensure accuracy, triplicate samples were utilized for the qRT-PCR analysis. Melting curve analysis of qRT-PCR products was performed to ensure the specificity of PCR amplification. The $2^{-\Delta\Delta Ct}$ method was used to calculate relative expression of *PcRan* (Livak and Schmittgen 2001).

Analysis of PcRan mRNA expression pattern after infection with pathogenic microorganisms

Experiments were conducted using previously acclimated, healthy, pathogen-free crayfish as described in the "Experimental red swamp crayfish and feeding methods" section, with feeding stopped 3 days before the start of the experiment. In the experiment, *P. clarkii* were randomly divided into three groups: a control group injected with phosphate buffer saline (PBS) and two experimental groups infected with WSSV or *A. veronii*. Each treatment was performed in triplicate with 30 crayfish in each group. White spot syndrome virus and *A. veronii* were previously stored in our laboratory. Pathogens were prepared as described

Table 1 Primers used for cloning and real-time polymerase chain reaction (PCR) in this study

Primers	Sequences (5′ → 3′)	Usage	Fragment size
Ran-F1	ATGGCAGCCGAGCAAGAA	ORF amplification	648 bp
Ran-R1	TTACAAATCTTCATCGTCCTCTGG		
Ran-3′ -Out	AAAGCAAAGTCCATCATTTTCCATA	3′ RACE	
Ran-3′ -In	CCAGTGGCAGCAACAAATCGA		
Ran-5′ -Out	CATTGAATTTTATAGGACCTCTGTT	5′ RACE	
Ran-5′ -In	TGTAGCAACATATTTCTTTTCAAA		
3′ RACE Olig (T)- Adaptor	CTGATCTAGAGGTACCGGATCC$(T)_{14}$	Adaptor Primer for RACE	
3′ RACE Adaptor	CTGATCTAGAGGTACCGGATCC		
5′ RACE Olig (T)- Adaptor	GACTCGAGTCGACATCGA$(T)_{17}$		
5′ RACE Adaptor	GACTCGAGTCGACATCG		
Ran-F2	GCAAGGTCAAAGCAAAGTCCA	qRT-PCR	127 bp
Ran-R2	TCACCAATCAGTTTACGTGCAAG		
18S-F1	ACCGATTGAATGATTTAGTGAG		129 bp
18S-R1	TACGGAAACCTTGTTACGAC		
Ran-F3	CCGGAATTCATGGCAGCCGAGCAAG(*EcoR* I)	Overexpression	
Ran-R3	CCGCTCGAGCAAATCTTCATCGTCCTCTGG(*Xho* I)		
Ran-F4	ACGCGTCGACATGGCAGCCGAGCAAG(*Sal* I)		
Ran-R4	CGCGGATCCCAAATCTTCATCGTCCTCTGG(*Hind* III)		

previously. Briefly, *A. veronii* and WSSV were extracted from naturally infected crayfish tissues and gills, and then, bacterial and viral suspensions were prepared (Zhu et al. 2022). For the WSSV-infected group, each crayfish was injected with 100 μL of WSSV inoculum (approximately 1×10^7 copy number) through the second and third abdominal segments. For the *A. veronii*-infected group, 100 μL of *A. veronii* inoculum was administered (approximately 6.04×10^6 colony-forming units (CFU)/crayfish). Crayfish in the PBS control group were injected with an equal amount of sterile PBS per crayfish. The hepatopancreas, gills, intestines, and hemocytes were sampled from randomly collected nine crayfishes (three from each replicate) from each group at 3, 6, 12, 24, 36, and 48 h post-injection for RNA extraction and qRT-PCR. The qRT-PCR steps were carried out as described in Sect. "Tissue distribution of PcRan".

For hemocytes extraction, pre-cooled hemolymph anticoagulant (336 mmol/L sodium chloride, 27 mmol/L sodium citrate, 9 mmol/L EDTA, 115 mmol/L glucose, and pH 7.2) was used to extract hemolymph from the pericardial cavity of crayfish. The sample was then centrifuged at $400\times g$ for 10 min to obtain hemocytes. To ensure accuracy, triplicate samples were analyzed for each treatment.

Expression of recombinant PcRan and eukaryotic plasmid construction

The forward and reverse primers *Ran*-F3 and *Ran*-R3 (Table 1), respectively, were used to clone *PcRan* (restriction sites are represented by underlined letters). Subsequently, the *PcRan* sequence was inserted into the His-tag pET-32a (+) vector. Briefly, the target fragment recovered from the gel and pET-32a (+) was double digested separately. The recombinant plasmid was ligated with T4 ligase (Takara, Japan) in a metal bath at 16 °C overnight, and the heat shock method was used to transform the ligation product into DH5α competent cells. Next to grow the culture strain, the bacterial solution was spread evenly on Luria–Bertani (Amp^+) solid medium and positive clones were selected for sequencing. The plasmid of the correctly sequenced strain was transformed into BL21 (DE3) competent cells according to the above method.

The coding region was amplified using the specific primers *Ran*-F4 and *Ran*-R4 (Table 1). The purified PCR products and expression vector pEGFP-N3 (Invitrogen, USA) were digested with restriction endonucleases *Sal* I and *Hind* III. Then, the recombinant plasmid was transformed into DH5α competent cells, the positive clone strains selected for sequencing, and the correctly sequenced strain named as pEGFP-N3-Ran and frozen for later use (Gao et al. 2023).

Purification of rPcRan protein and preparation of mouse anti-PcRan polyclonal antibodies

Transformed *Escherichia coli* cells were cultured at 37 °C until the absorbance at optical density 600 nm (OD_{600}) reached 0.6. Once this threshold was reached, protein expression was induced for 6 h at 37 °C by adding 1.0 mM isopropyl-β-D-thiogalactopyranoside (IPTG) (Sigma, USA). Then, the sample was centrifuged at $8000\times g$ for 10 min at 4 °C to collect the bacteria. The bacteria were suspended in pre-cooled lysis buffer and the precipitate collected after ultrasonic crushing (power, 35%; ultrasonic pulse, 3 s; total time, 30 min). Subsequently, rPcRan was cleaved with 8 M urea, and the recombinant protein was purified using Ni-IDA affinity chromatography. Impure proteins were washed with protein binding buffer and recombinant proteins eluted with elution buffer (20 mM Tris, 50

mM NaCl, 2 M urea, and 20–100 mM imidazole). The protein eluate was dialyzed against a dialysate at 4 °C to remove urea and imidazole, and the protein was concentrated by ultrafiltration centrifugation. After the purified protein was detected using sodium dodecyl-sulfate polyacrylamide gel electrophoresis (SDS-PAGE), the protein concentration was determined using the bicinchoninic acid method.

We prepared polyclonal antibodies according to previously reported methods (Zhao et al. 2023b). First, mice were injected intraperitoneally with Freund's complete adjuvant emulsified protein (100 µL Freund's complete adjuvant + 100 µL purified protein). Mice were immunized twice. The emulsified protein in Freund's incomplete adjuvant (100 µL Freund's incomplete adjuvant + 100 µL purified protein) was injected every other week for a total of two immunizations. Finally, the mice were sacrificed at the 5th week, and the eyeballs were removed to collect serum. The serum was frozen and stored at − 80 °C till analysis.

Enzyme linked immunosorbent assay (ELISA) analysis

The indirect ELISA method was used to detect the PcRan antibody titer according to a previously reported method (Wang et al. 2023). Briefly, diluted proteins were coated with 2 × coating buffer (50 mM Na_2CO_3, 50 mM $NaHCO_3$, pH 9.6) in 96-well plates (Corning, USA) overnight and then blocked with Tris-buffered saline with Tween® 20 containing 10% (w/v) skimmed milk powder for 2 h. Subsequently, an antibody serum was used as the primary antibody, serially diluted, and incubated at 37 °C for 2 h. Unimmunized mouse serum was used as a control. The plates were washed three times with washing solution. Then, goat anti-mouse IgG (H + L) (Beyotime, China), diluted at a ratio of 1:1000, was used as the secondary antibody and incubated at 37 °C for 1 h. The plates were washed three times with washing solution. Finally, 3,3′,5,5′-tetramethylbenzidine single-component chromogenic solution (Solarbio, Beijing, China) was used for color development, and an equal volume of 1 M hydrochloric acid or sulfuric acid solution was added to terminate the reaction. A microplate reader (PerkinElmer, USA) was used to measure the absorbance at an optical density of 450 nm (OD_{450}).

Western blot (Wb) analysis

To verify whether the prepared polyclonal antibody can recognize and bind endogenous PcRan, we examined it using Wb. Briefly, after the target protein was separated by 12.5% SDS-PAGE, the target protein was transferred to a polyvinylidene difluoride (PVDF) membrane (Millipore, USA). The membrane was blocked with 5% skim milk in TBS containing 0.1% Tween. Anti-PcRan antibody or control mouse serum was used as the primary antibody for detection. Horseradish peroxidase-labeled anti-mouse IgG (Beyotime Biotechnology, China) was used as the secondary antibody and incubated at 37 °C for 1 h (Wang et al. 2015). Finally, ECL luminescent solution (Sigma, USA) was used for color development and a gel imaging system (Bio-Rad, USA) was used to observe the protein bands.

Tissue protein samples were prepared according to the manufacturer's instructions and RIPA lysis buffer (Solarbio, Beijing, China) containing phenylmethanesulfonyl fluoride was used to extract proteins. Then, the bicinchoninic acid method was used to detect the protein concentration, and equal amounts of each tissue protein (100 µg) were taken

Fig. 1 **A** Full-length nucleotide and deduced amino acid sequences of PcRan. The G1, G2, G3, G4, and G5 motifs are marked in red, orange, yellow, green, and blue boxes, respectively. Start and stop codons are shaded in gray. The red and black fonts indicate the amino acid (XP_045614622.1) and nucleotide (XM_045758666.1) sequences, respectively. **B** Secondary structure elements, α-helices and β-strands, are represented in purple and green, respectively. **C** Domain organization of PcRan as predicted by SMART. **D** PcRan spatial model constructed based on 2n1b.1.A (GTP-binding nuclear protein Ran) using SWISS-MODEL software

for SDS-PAGE electrophoresis, and tissue distribution of PcRan was detected by the Wb method.

Overexpression of PcRan in vivo and bacterial clearance assay

Healthy crayfish were randomly injected with 100 μL (10 μg) of pEGFP-N3 plasmid, pEGFP-N3-Ran plasmid, or PBS to overexpress *PcRan*. Then, the gills, intestines, hemocytes, and hepatopancreas from five randomly selected crayfish from each group were used to detect the overexpression efficiency of the target gene in vivo at 0, 24, 48, and 72 h post infection. Nine crayfish were selected from each group and injected with plasmid or PBS as described above. Forty-eight hours after injection, each crayfish was injected with 100 μL *A. veronii* (6.04×10^6 CFU). One hour after bacterial infection, tissues such as the gills and hemocytes were collected under sterile conditions, and then, the number of bacteria was evaluated using the plate count method (Sun et al. 2022). The experiment was repeated three times.

Survival rate experiment

PcRan recombinant plasmid, empty plasmid, or PBS [100 μL (10 ng/μL)] was injected into *P. clarkii* (30 crayfish in each group). All three groups were then injected with the same amount of *A. veronii* dilution for infection. The number of crayfish surviving was recorded every 12 h until the survival number of one group of crayfish reached 0. Differences in survival rates were tested using the Kaplan–Meier method (log-rankχ^2 test) (Huang et al. 2022).

Statistical analysis

Data of all experiments were analyzed using the Statistical Package for the Social Sciences (SPSS) 18.0. The values are expressed as mean ± standard deviation. The Student's *t*-test was used to determine the statistical significance of differences between two groups. Differences between groups were assessed using one-way analysis of variance (ANOVA) and post hoc tests. Statistical significance was set at * $P < 0.05$ and ** $P < 0.01$.

Results

cDNA cloning and bioinformatic analysis of PcRan

Using cDNA from *P. clarkii* gills as a template, the full-length cDNA sequence of *PcRan* was successfully cloned. The results showed that *PcRan* cDNA was 1074 bp in length, the

A

```
1     agtcagtcggagtgaggagggcggaagatagaggcggtgcacgcgggcaaggaagaaaaac  60
61    ttaaagaatttgtggtgcccacatccagcacaATGGCAGCCGAGCAAGAAATGCCCACCT  120
1                                     M  A  A  E  Q  E  M  P  T      9
121   TTAAGCTGGTGTTGGTTGGTGATGGTGGTACTGGTAAAACCACATTTGTGAAAAGGCATT  180
10    F  K  L  V  L  V  G  D  G  G  T  G  K  T  T  F  V  K  R  H    29
181   TGACTGGCGAATTTGAAAAGAAATATGTTGCTACACTTGGGGTGGAAGTTCATCCTCTTG  240
30    L  T  G  E  F  E  K  K  Y  V  A  T  L  G  V  E  V  H  P  L    49
241   TATTCCACACTAACAGAGGTCCTATAAAATTCAATGTATGGGACACTGCAGGACAAGAAA  300
50    V  F  H  T  N  R  G  P  I  K  F  N  V  W  D  T  A  G  Q  E    69
301   AATTAGGGGGCCTTCGTGATGGTTACTACATTCAAGCTCACTGTGCCATTATTATGTTTG  360
70    K  L  G  G  L  R  D  G  Y  Y  I  Q  A  H  C  A  I  I  M  F    89
361   ATGTCACATCCAGAGTCACCTACAAAAATGTTCCTAACTGGCATAGAGATCTTGTGCGTG  420
90    D  V  T  S  R  V  T  Y  K  N  V  P  N  W  H  R  D  L  V  R    109
421   TATGCGAAAATATTCCCATTGTTTTGTGTGGAAACAAGGTTGATGTTAAAGATCGCAAGG  480
110   V  C  E  N  I  P  I  V  L  C  G  N  K  V  D  V  K  D  R  K    129
481   TCAAAGCAAAGTCCATCATTTTCCATAGAAAGAAGAATCTACAGTACTATGACATCTCTG  540
130   V  K  A  K  S  I  I  F  H  R  K  K  N  L  Q  Y  Y  D  I  S    149
541   CCAAGTCGAACTACAACTTCGAAAAACCTTTCCTGTGGCTTGCACGTAAACTGATTGGTG  600
150   A  K  S  N  Y  N  F  E  K  P  F  L  W  L  A  R  K  L  I  G    169
601   ACCCCAACCTAGAATTTGTTGCGATGCCTGCACTCCTGCCACCAGAGGTACAAATGGACC  660
170   D  P  N  L  E  F  V  A  M  P  A  L  L  P  P  E  V  Q  M  D    189
661   CCCAGTGGCAGCAACAAATCGAGAACGATCTCCAAGTAGCTTCCCAGACTGCTTTACCAG  720
190   P  Q  W  Q  Q  Q  I  E  N  D  L  Q  V  A  S  Q  T  A  L  P    209
721   AGGACGATGAAGATTTGTAAagctaaccactgtattgcagacaaaataaagcttatattt  780
210   E  D  D  E  D  L  *                                          215
781   gttaaaactgtgttgaattggaattgtttaaaacatgccctcatcttttgctattgaaac  840
841   ttgctctatgaaggctttgatttttgttttcatataaatgacgaagtggctacatttaca  900
901   tatttgcttgcacgtggatcattcaacagcgtgcttgtgtaaaacattcctatatgcatg  960
961   ctgctagtggtaaaggaactaaacattggaaatattttcaacatataagcctacggttac 1020
1021  tgttatacaaaatttttctaataaactgaagaaatccaaaaaaaaaaaaaaaaaa      1074
```

B

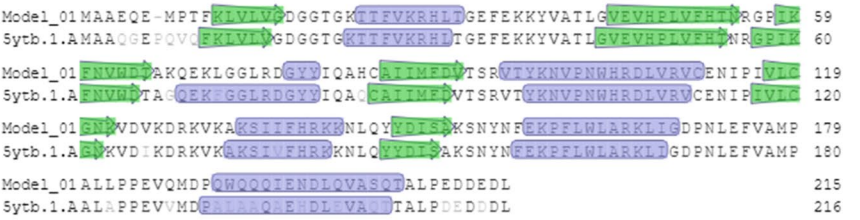

C

D

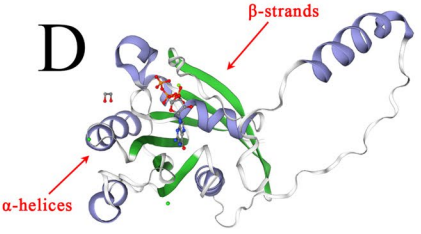

ORF sequence was of 648 bp, 214 amino acids were encoded, the 3′ and 5′-untranslated regions were 92 and 334 bp in length, respectively, and the predicted molecular size was 24.62 kDa (Fig. 1A). The spatial structure model of the PcRan protein obtained using the SWISS-MODEL software showed that PcRan contained multiple α-helices and β-strands (Fig. 1B). SMART online software prediction results showed that the PcRan amino acid sequence contained a conserved RAN domain (Fig. 1C). The predicted 3D structure of PcRan was based on the model 2n1b.1.A (GTP-binding nuclear protein Ran) with a sequence identity of 88.84% (Fig. 1D).

PcRan amino acid multiple sequence alignment and homology analysis

To study the evolution of the PcRan protein, we compared the Ran sequences of other species in GenBank with the PcRan sequences. The multiple alignment results revealed that the Ran protein is relatively conserved in different species, exhibiting a conserved G domain. The G domain is conserved across the RAS superfamily, and consists of five motifs (G boxes) (Fig. 2). To analyze the evolutionary relationship between PcRan and Ran of other species, a phylogenetic tree was established using the neighbor-joining method. The software MEGA 8.0 was used to analyze phylogenetic relationships of the PcRan amino acid sequences (Fig. 3). The results showed that PcRan was clustered into a small branch with Ran of *Penaeus monodon*, *Penaeus vannamei*, *P. japonicus*, and *M. rosenbergii*, and they were closely related.

Distribution of PcRan in tissues of healthy crayfish

The level of *PcRan* mRNA relative to that of 18S RNA in different tissues of crayfish was determined using qRT-PCR. The results showed that *PcRan* was expressed in all tissues of crayfish and exhibited tissue-specific expression. Presence was mainly observed in the muscle, gills, and intestines of unchallenged crayfishes, whereas levels were relatively poor in the hepatopancreas and gonads (Fig. 4). Western blotting was used to detect the expression of PcRan protein. The results showed that its expression pattern at the protein level was similar to that at the mRNA level.

Time course analysis of PcRan upon microbial challenge

We used the qRT-PCR method to analyze the mRNA expression of PcRan in the gills, hemocytes, hepatopancreas, and intestines after 3, 6, 12, 24, 36, and 48 h of inoculation. The expression of *PcRan* in the gills, hemocytes, hepatopancreas, and intestines began to change significantly ($P < 0.05$) after 3 h in the group injected with *A. veronii* compared with the control group (Fig. 5). The expression level of *PcRan* in the gills of crayfishes infected with *A. veronii* showed a rapid increase, peaking at 12 h, after which the expression level began to decrease (Fig. 5A). In hemocytes, the expression level of *PcRan* first decreased at 6 h and was significantly different compared with the control ($p < 0.01$), and then reached a peak at 12 h and 24 h (Fig. 5B). The expression of *PcRan* in the hepatopancreas rapidly increased after 6 h, further exhibiting a trend of first significantly ($p < 0.01$) decreasing and then increasing, peaking at 48 h (Fig. 5C). The expression level in the intestine was similar to that in hemocytes, with a significant decrease at 6 h and a peak at 24 h (Fig. 5D). Figure 6 shows that, after infection

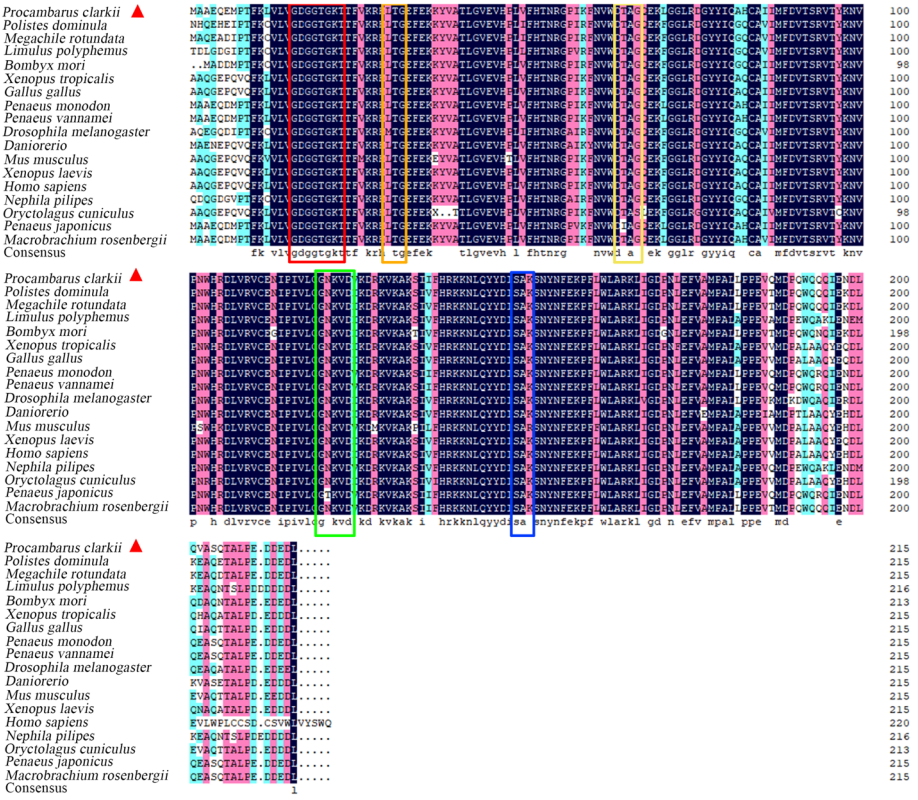

Fig. 2 Amino acid multiple sequence alignment of PcRan and other species. All species contain a conserved G domain, which consisted of five G motifs. Different colors represent the different motifs. For details, see Fig. 1. The amino acid sequence accession numbers used were: *Polistes dominula* (XP_015182751.1), *Megachile rotundata* (XP_012154527.1), *Limulus polyphemus* (XP_022245563.1), *Bombyx mori* (NP_001040274.1), *Xenopus tropicalis* (NP_001004829.1), *Gallus gallus* (NP_990589.1), *Penaeus monodon* (XP_037799067.1), *Penaeus vannamei* (XP_027236905.1), *Drosophila melanogaster* (NP_001285112.1), *Danio rerio* (XP_005173151.1), *Mus musculus* (AAA64248.1), *Xenopus laevis* (NP_001128547.1), *Homo sapiens* (XP_016875261.1), *Nephila pilipes* (GFU02971.1), *Oryctolagus cuniculus* (XP_008260588.1), *Penaeus japonicus* (AAY96645.1), and *Macrobrachium rosenbergii* (AND76907.1)

with WSSV, the expression of *PcRan* in the gills generally exhibited an upward trend, and showed a trend of first significantly increasing and then decreasing, with the highest expression level at 12 h (Fig. 6A). However, in the hemocytes, *PcRan* exhibited a downward trend, with the lowest expression appearing at 36 h; the expression level was significantly higher than that of the control group at 48 h ($P < 0.05$) (Fig. 6B). In the hepatopancreas, the mRNA level of *PcRan* showed a rapid increase after 3 h; subsequently, a trend of marked reduction followed by an increase was observed (Fig. 6C). In the intestine, the expression levels of *PcRan* in the WSSV-infected group at different time points were significantly higher than those of the control group ($p < 0.01$), and the expression levels at different time points were approximately the same. The expression of *PcRan* began to decline at 48 h after infection (Fig. 6D).

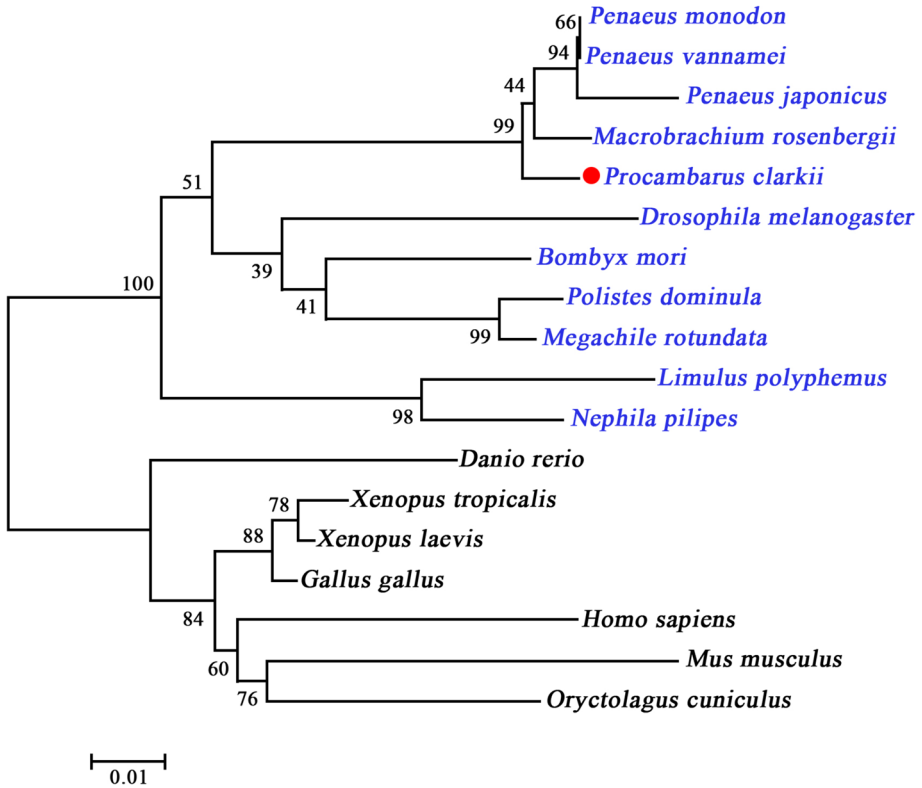

Fig. 3 Species phylogenetic tree constructed based on Ran amino acid sequence. Blue and black fonts represent the two major groups, respectively. The serial numbers of different species in the evolutionary tree are: *Penaeus monodon* (XP_037799067.1), *Polistes dominula* (XP_015182751.1), *Megachile rotundata* (XP_012154527.1), *Bombyx mori* (NP_001040274.1), *Drosophila melanogaster* (NP_001285112.1), *Limulus polyphemus* (XP_022245563.1), *Nephila pilipes* (GFU02971.1), *Macrobrachium rosenbergii* (AND76907.1), *Penaeus vannamei* (XP_027236905.1), *Penaeus japonicus* (AAY96645.1), *Danio rerio* (XP_005173151.1), *Xenopus tropicalis* (NP_001004829.1), *Xenopus laevis* (NP_001128547.1), *Gallus gallus* (NP_990589.1), *Homo sapiens* (XP_016875261.1), *Mus musculus* (AAA64248.1), *Oryctolagus cuniculus* (XP_008260588.1)

rPcRan protein expression and preparation of mouse anti-PcRan polyclonal antibodies

We inserted the PcRan sequence into the pET-32a (+) vector to construct a prokaryotic expression vector to express the rPcRan protein. According to the results of SDS-PAGE, rPcRan exhibited a distinct band at 43 kDa (Fig. 7); this molecule size included 24.62 kDa of rPcRan proteins and Trx-His-tag proteins. The protein expression was the highest when the final concentration of isopropyl-β-D-thiogalactopyranoside was 1 mM and induced for 6 h. After ultrasonic crushing, the recombinant protein was found to mainly exist in the bacterial pellet.

Next, we prepared rPcRan polyclonal antibodies to detect the biological function of PcRan. The concentration of the purified ultrafiltered protein was adjusted to 1 mg/mL and mice were immunized. The eyeballs of the immunized mice were removed to collect blood, and the antibodies in the obtained samples were detected using ELISA and Wb. The

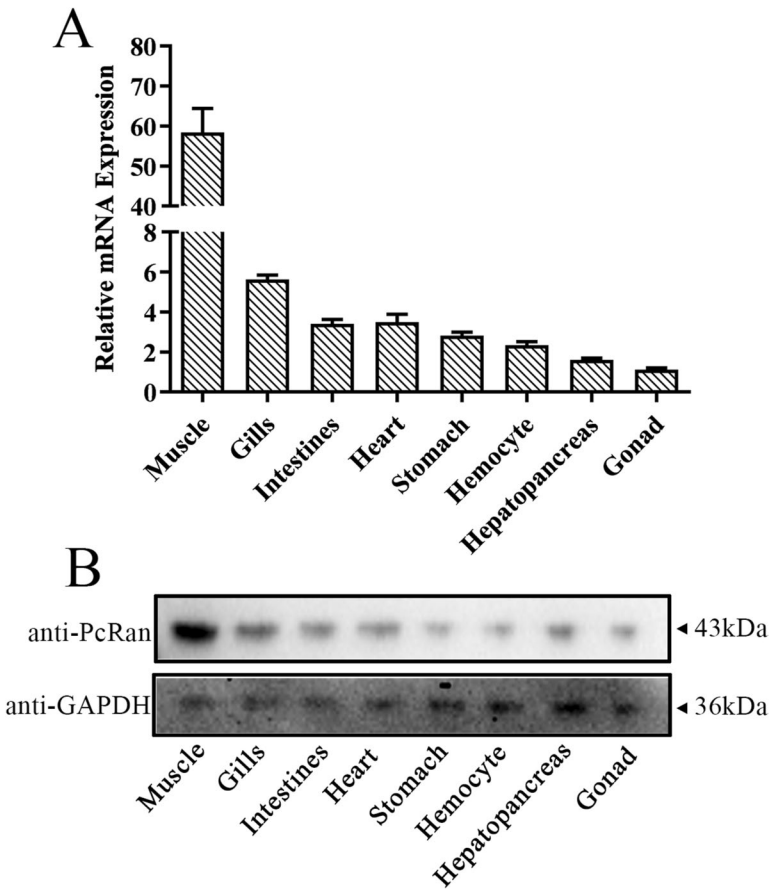

Fig. 4 **A** Expression of *PcRan* in different tissues of crayfish. The mRNA expression level was determined by qRT-PCR with 18S rRNA as the reference gene. Bars represent the mean ± S.E. ($n = 5$). **B** The protein expression levels of PcRan are based on the western blotting method. PcRan protein was detected using GAPDH as the internal reference

ELISA results revealed that the serum titer was as high as 1/90,000 (Table 2), indicating that highly efficient antibodies were prepared. Results of Wb revealed that the antibody could specifically recognize endogenous Ran in crayfish (Fig. 8). The successful development of antibodies provides useful tools for protein detection and functional research.

3.6 Detection of PcRan overexpression efficiency and its involvement in the immune response against *A. veronii* infection

PcRan was overexpressed using the pEGFP-N3-Ran plasmid. Compared with the pEGFP-N3 empty plasmid group, after injection of the overexpression plasmid, the mRNA expression of *PcRan* in different tissues was significantly increased (Fig. 9A, 9B). Forty-eight hours after the injection of the recombinant plasmid, a noticeable increase was observed in the expression level in the gills, which was approximately five times higher than that of the

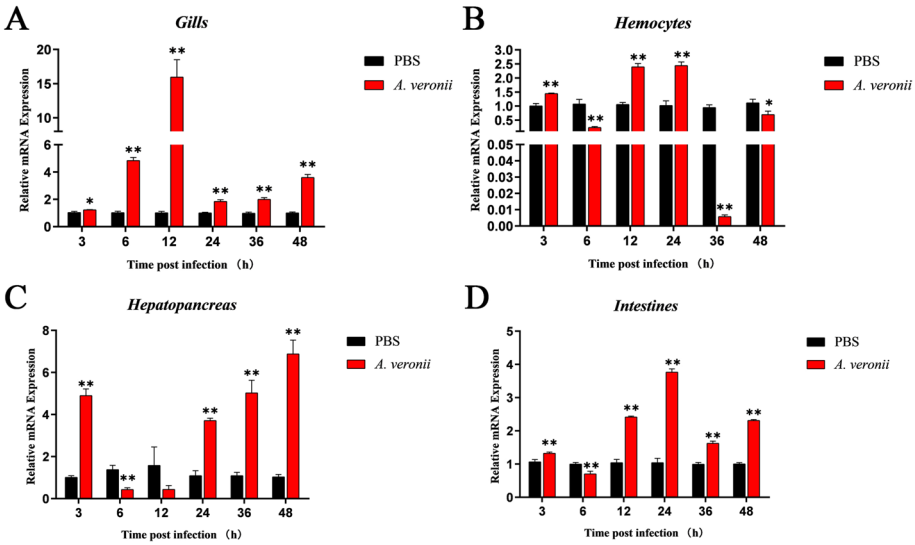

Fig. 5 Expression levels of *PcRan* in the gills (**A**), hemocytes (**B**), hepatopancreas (**C**), and intestines (**D**) of *Procambarus clarkii* upon *Aeromonas veronii* infection. Data are presented as mean ± SEM ($n = 5$). * $P < 0.05$, ** $P < 0.01$

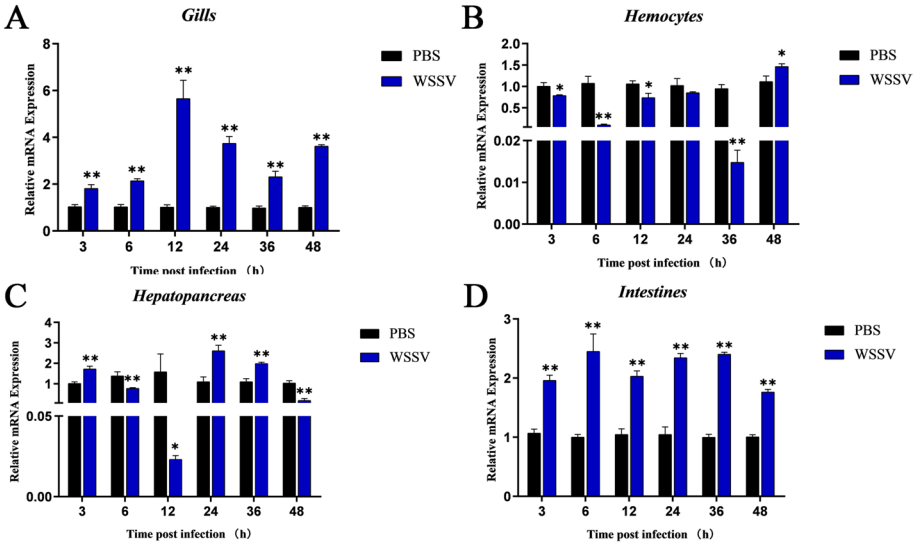

Fig. 6 Expression levels of *PcRan* in the gills (**A**), hemocytes (**B**), hepatopancreas (**C**), and intestines (**D**) of *Procambarus clarkii* upon white spot syndrome virus (WSSV) infection. Data are presented as mean ± SEM (n = 5). * $P < 0.05$, ** $P < 0.01$

control group. Additionally, a significant increase was observed in the expression level of PcRan in the hemocytes. However, it is worth noting that the expression level in the gills began to decrease at 72 h, whereas the expression level in hemocytes continued to increase.

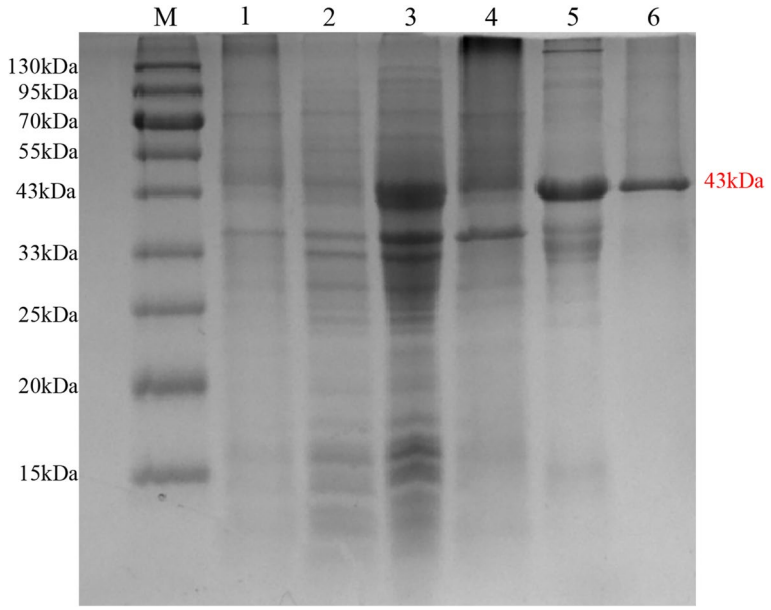

Fig. 7 Sodium dodecyl-sulfate polyacrylamide gel electrophoresis revealed the expression level of PcRan recombinant protein. M: Marker; lanes 1–6 represent pET-32a (+) empty plasmid, uninduced bacterial liquid, 1 mM isopropyl-β-D-thiogalactopyranoside (IPTG)-induced bacterial liquid, induced bacterial supernatant, induced bacterial pellet, and purified rPcRan, respectively

Table 2 Indirect enzyme linked immunosorbent assay (ELISA) analysis of titers of anti-PcRan polyclonal antibody (P/N > 2 is positive)

Dilution ratio of serum	Absorbance at OD_{450} nm of positive serum (P)	Absorbance at OD_{450} nm of negative serum (N)	P/N
100	1.665	0.143	11.64
1000	1.869	0.059	31.68
10,000	1.406	0.046	30.57
30,000	0.932	0.047	19.83
90,000	0.278	0.046	6.04
270,000	0.066	0.046	1.43
810,000	0.049	0.046	1.07
2,430,000	0.045	0.050	0.90

To ensure the overexpression efficiency in different tissues, we unified the subsequent sampling time to 48 h. At the same time, Wb revealed the protein expression of various tissues, and the results were consistent with the results of mRNA expression (Fig. 9C). These results imply that the vector was well-designed and can achieve the purpose of overexpressing PcRan. We conducted a bacterial clearance experiment to test whether *PcRan* can prevent *A. veronii* colonization. The results showed that after overexpression of *PcRan*, the number of bacteria in different tissues in vivo was significantly reduced compared with the control group (Fig. 10). This shows that overexpression of *PcRan* improves the bacterial

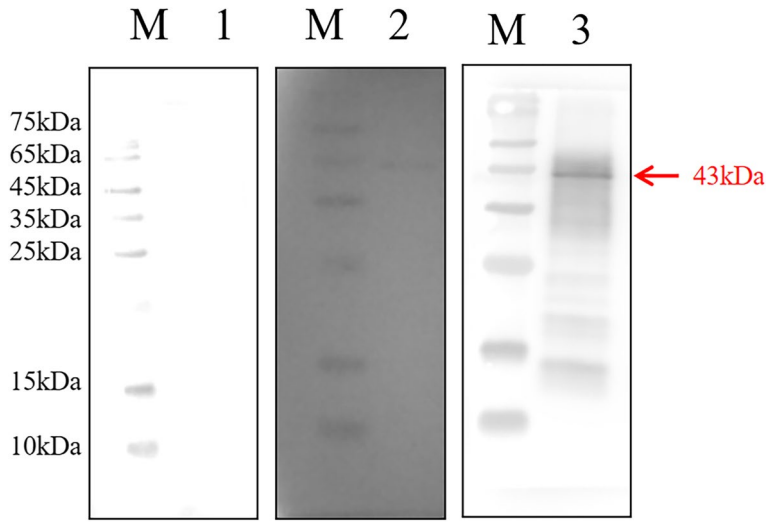

Fig. 8 Western botting analysis of rPcRan using different antibodies. M, marker; lane 1, negative serum; lane 2, mouse anti-His tag antibody; and lane 3, mouse anti-PcRan polyclonal antibodies

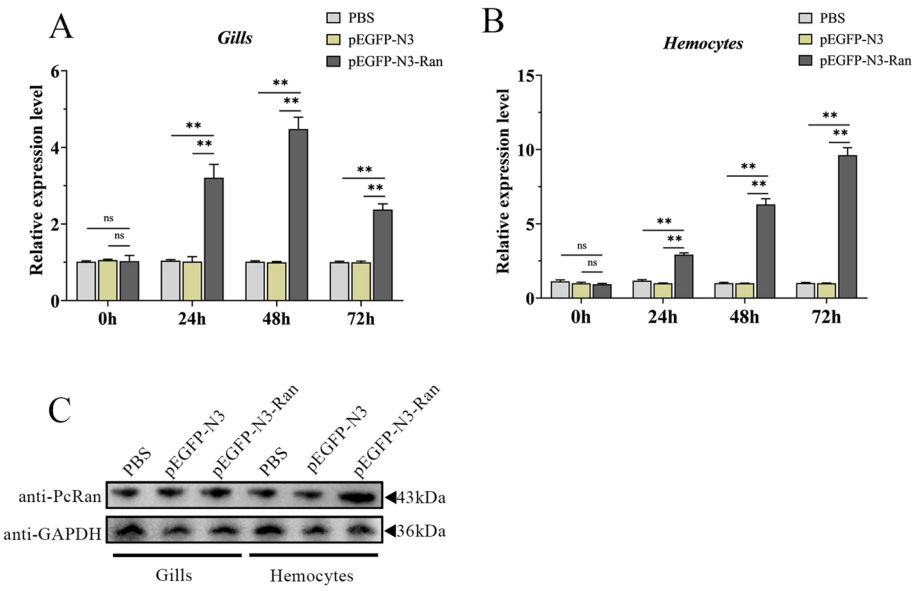

Fig. 9 Effects of pEGFP-N3-Ran injection on the expression of PcRan. The relative expression of PcRan mRNA was measured in the gills (**A**) and hemocytes (**B**) at 24, 48, and 72 h after injection of pEGFP-N3-Ran. Bars represent mean ± S.E. ($n = 5$). **C** Protein expression of PcRan. The protein expression level of different tissues was detected using western blotting after the crayfish were injected with the pEGFP-N3-Ran plasmid

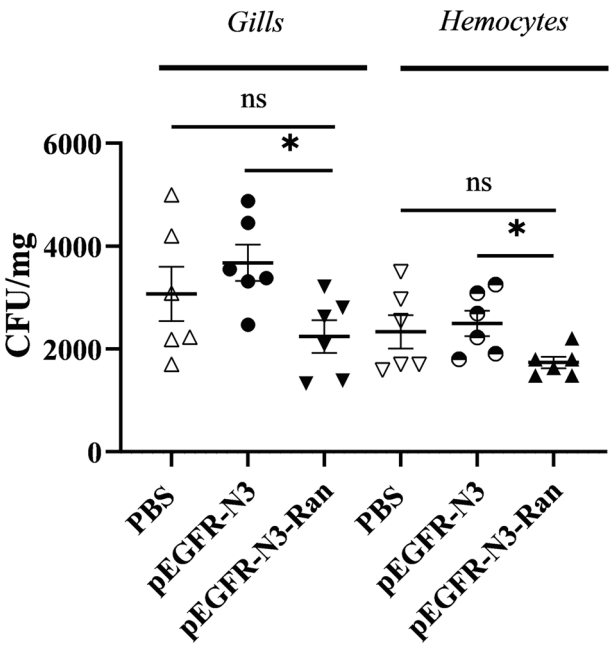

Fig. 10 *PcRan* prevents *Aeromonas veronii* colonization in vivo. Bacterial burdens in the gills and hemocytes in different groups infected with *A. veronii*. Data are analyzed statistically using one-way analysis of variance (ANOVA) and post hoc tests (ns, no significant change, * $P < 0.05$)

clearance ability in the crayfish. Taken together, *PcRan* may play an important role in limiting bacterial infections in vivo.

Subsequently, a survival rate experiment was conducted. The *PcRan* recombinant plasmid, empty plasmid, or PBS was injected into *A. veronii*-infected crayfish. Subsequently, surviving of *P. clarkii* were counted. At 84 h after bacterial infection, the cumulative survival rate of the pEGFP-N3-Ran group was 30%, whereas the survival rates of the PBS and pEGFP-N3 groups were 0% and 13.333%, respectively. This shows that the survival rate of crayfish can be improved by increasing the activity of *PcRan* (Fig. 11).

Discussion

Small GTPases are crucial for various intracellular processes, encompassing signal transduction, cell proliferation, cytoskeletal arrangement, and internal membrane trafficking. Immune signal transduction factors are one of the three major immune factors along with pattern recognition proteins and their receptors and immune response factors. In addition to the heterotrimeric G proteins involved in signal transduction, small G proteins are present that function in monomeric form within cells. Ran is a signal transduction factor in the form of small G proteins (Han 2012). Similar to other Ran protein structures, PcRan contained a highly conserved G domain, and had a complete G domain consisting of G1–G5 motifs. In the present study, the obtained PcRan exhibited structural characteristics similar to those of Ran from mammals, fishes, and other invertebrates, indicating that Ran is highly conserved among different species.

In *Larimichthys crocea* (Han 2012), *Ran* mRNA levels were detected at varying degrees in all tested tissues such as the kidney and liver. In *P. monodon* (Zhou et al. 2012), *PmRan* mRNA was present in all tested tissues, with the highest level in the ovary. In the present

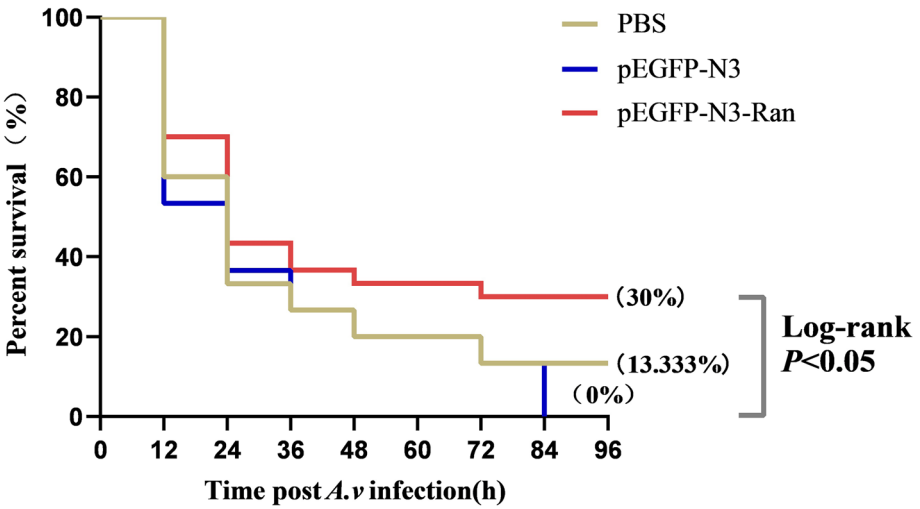

Fig. 11 Percent survival of crayfish after *Aeromonas veronii* infection. The number of dead crayfish was counted every 12 h. Differences in cumulative mortality levels between groups were analyzed using the log-rank χ^2 test

study, *PcRan* mRNA was expressed in different tissues of crayfish, with the highest expression levels in the muscle and gills. Gills are the main respiratory-related organs of aquatic crustaceans and thus play an important role in regulating external osmotic pressure, ion transport, and immune responses (Thabet et al. 2017; Bao et al. 2019). The ubiquitous expression pattern in this tissue is consistent with the expression pattern of *P. monodon* Ran and *M. rosenbergii* Ran, both of which showed tissue-specific expression (Zhou et al. 2012; Ning et al. 2017).

Ran participates in the immune response of aquatic animals. In the present study, to observe whether *PcRan* in crayfish was involved in the immune response against WSSV and *A. veronii*, changes in mRNA expression patterns in four major immune organs following pathogen infection were studied. The results revealed that after pathogenic infection, the transcript level of *PcRan* varied in a time-dependent manner in different tissues. We speculate that the emergence of different expression patterns may be related to the time when immune organs function sequentially. Other studies revealed that after inoculation with polyinosinic:polycytidylic acid (Poly I:C), and bacterial lipopolysaccharides, *Ran* in the blood, liver, and spleen of *L. crocea* (Han 2012) was significantly upregulated. After stimulation of *Marsupenaeus japonicus* (Han et al. 2012) with WSSV, the expression of Ran-iso was significantly changed, indicated that it plays an important role in immune function. These findings suggest that *PcRan* may be critical for immune regulation during crayfish pathogen infection. To confirm these findings, it is crucial to conduct a more comprehensive investigation into the function aspects of the gene.

We constructed a eukaryotic expression vector of *PcRan* to achieve overexpression of *PcRan*. After injection of the recombinant plasmid, the expression level of *PcRan* could be upregulated in both the gills and hemocytes. Subsequently, we studied the ability of crayfish overexpressing *PcRan* to clear *A. veronii* in vivo and whether this overexpression could improve the survival rate of crayfish when exposed to *A. veronii*. The results showed that after *PcRan* overexpression, the number of bacteria in crayfish was significantly reduced, the survival rate was significantly improved, and the crayfish was protected against *A.*

veronii infection. This is consistent with results reported in the literature. Some small G proteins, including the Rho GTPase family and the Rab GTPase family, were found to be related to phagocytosis (Wu et al. 2008; Mao and Finnemann 2015). Moreover, *PjRan* was further demonstrated to regulate hemocyte phagocytosis in shrimp to combat viral infection through direct interaction with the myosin light chain (Liu et al. 2009). Overexpression of *PjRan* led to a significant reduction in virus copy number. After *PjRan* interference, the virus copy number in shrimp significantly increased. In contrast, after interference with *MrRan*, a marked decrease was observed in the copy number of *S. eriocheiris* and death rate in prawn (Ning et al. 2017). The differences in these results may be related to their different pathogen infection mechanisms and the innate immunity of shrimp. However, these experimental results demonstrate that Ran can participate in the immune process of the body in response to pathogen infection through phagocytosis. In the present study, the over-expression of *PcRan* may improve the phagocytosis activity of hemocytes. Therefore, the phagocytosis rate of pathogens was increased and the survival rate of crayfish was also enhanced.

The subcellular location of a protein is often related to its molecular structure and function. Therefore, we need to further study the subcellular localization of *PcRan* in cells to provide research directions for understanding the immune mechanism of Ran. The mechanism of *PcRan* resistance to bacterial infection is also a limitation of our study. In the next step, we aim to focus on the antibacterial immune defense mechanism of *PcRan*. We hope that our research can provide insights into the mechanisms of immunity and disease resistance in *P. clarkii*.

In summary, we report *Ran* in *P. clarkii*. Ran can be detected in various tissues of crayfish. In addition, *PcRan* is involved in the immune process of crayfish in response to disease infections. The overexpression of *PcRan* further suggests that *PcRan* can effectively prevent the colonization of *A. veronii* in crayfish and improve the survival rate of the crayfish. Our results further confirmed that Ran has immune functions. This research result can provide a basis for further research on the specific immune mechanism of *PcRan* against bacterial infection, and can also better understand and reveal the immune mechanism of invertebrates.

Author contribution Yanlong Gu: software, investigation, data, writing original draft, writing—review and editing. Lei Zhu: conceptualization, supervision, methodology, software, resources, data curation, funding acquisition, visualization. Tong Zhao: software, investigation, data, visualization, validation. Xinru Wang: methodology. Hao Li: validation, Libo Hou: validation. Xianghui Kong: conceptualization, supervision, methodology, software, resources, data curation, visualization.

Funding This article was supported by the National Natural Science Foundation of China (NO. 32202968).

Data availability The datasets used or analyzed during the current study are available from the corresponding author on reasonable request.

Declarations

Competing interests The authors declare no competing interests.

Ethics approval The study was performed in strict compliance with the recommendations set forth in the Animal Ethics Procedures and Guidelines of the People's Republic of China. All animal protocols were approved by the Animal Administration and Ethics Committee of Henan Normal University (Approval no: HNSD-2024-BS-0130).

Conflict of interest The authors declare no competing interests.

References

Ach RA, Gruissem W (1994) A small nuclear GTP-binding protein from tomato suppresses a *Schizosaccharomyces pombe* cell-cycle mutant. Proc Natl Acad Sci USA 91:5863–5867

Bao J, Xing YN, Jiang HB, Li XD (2019) Identification of immune-related genes in gills of Chinese mitten crabs (*Eriocheir sinensis*) during adaptation to air exposure stress. Fish Shellfish Immunol 84:885–893

Bischoff FR, Ponstingl H (1991) Mitotic regulator protein RCC1 is complexed with a nuclear ras-related polypeptide. Proc Natl Acad Sci USA 88:10830–10834

Clarke PR, Zhang C (2001) Ran GTPase: a master regulator of nuclear structure and function during the eukaryotic cell division cycle? Trends Cell Biol 11:366–371

Drivas GT, Shih A, Coutavas E, Rush MG, D'Eustachio P (1990) Characterization of four novel ras-like genes expressed in a human teratocarcinoma cell line. Mol Cell Biol 10:1793–1798

Fu X, Guo M, Liu J, Li C (2023) circRNA432 enhances the coelomocyte phagocytosis via regulating the miR-2008-ELMO1 axis in Vibrio splendidus-challenged *Apostichopus japonicus*. Commun Biol 6:115

Gao F, Shi X, Zhao Y, Qiao D, Pei C, Li C, Zhao X, Kong X (2023) The role of *Cc*PTGS2a in immune response against *Aeromonas hydrophila* infection in common carp (*Cyprinus carpio*). Fish Shellfish Immunol 141:109058

Gu Y, Zhu L, Wang X, Li H, Hou L, Kong X (2023) Research progress of pattern recognition receptors in red swamp crayfish (*Procambarus clarkii*). Fish Shellfish Immunol 141:109028

Han F, Zhang X (2007) Characterization of a ras-related nuclear protein (Ran protein) up-regulated in shrimp antiviral immunity. Fish Shellfish Immunol 23:937–944

Han F, Wang X, Wang Z (2012) Molecular characterization of a Ran isoform gene up-regulated in shrimp immunity. Gene 495:65–71

Han F (2012) Molecular characterizations and functions of Ran, Rab, Rac in large yellow croaker. Dissertation, Hunan Agricultural University

Hetzer M, Gruss OJ, Mattaj IW (2002) The Ran GTPase as a marker of chromosome position in spindle formation and nuclear envelope assembly. Nat Cell Biol 4:E177–E184

Huang AG, He WH, Zhang FL, Wei CS, Wang YH (2022) Natural component geniposide enhances survival rate of crayfish *Procambarus clarkii* infected with white spot syndrome virus. Fish Shellfish Immunol 126:96–103

Kumar S, Stecher G, Tamura K (2016) MEGA7: molecular evolutionary genetics analysis version 7.0 for bigger datasets. Mol Biol Evol 33:1870–1874

Li CJ, Liu J, Gui JF (2006) cDNA cloning of Ran gene and analyses on its expression characterization and role in sperm nuclei decondensation in vitro in gibel carp *Carassius auratus gibelio*. J Fish China 03:297–304

Li CJ, Liu J, Shi YH, Yang ST, Gui JF (2003) Full length cDNA cloning and tissue expression specificity of Ran gene in *Color Crucian Carp*. Zool Res 1(03):173–179

Liu W, Han F, Zhang X (2009) Ran GTPase regulates hemocytic phagocytosis of shrimp by interaction with myosin. J Proteome Res 8:1198–1206

Livak KJ, Schmittgen TD (2001) Analysis of relative gene expression data using real-time quantitative PCR and the 2(-Delta Delta C(T)) Method. Methods 25:402–408

Lundin MH, Mikkelsen B, Gudim M, Syed M (2000) The structure and expression of the *Salmo salar* Ran gene. DNA Seq 11:41–50

Mao Y, Finnemann SC (2015) Regulation of phagocytosis by Rho GTPases. Small GTPases 6:89–99

Mattaj IW, Englmeier L (1998) Nucleocytoplasmic transport: the soluble phase. Annu Rev Biochem 67:265–306

Moore JD (2001) The Ran-GTPase and cell-cycle control. BioEssays 23:77–85

Ning M, Xiu Y, Yuan M, Bi J, Liu M, Wei P, Yan Y, Gu W, Wang W, Meng Q (2017) Identification and function analysis of ras-related nuclear protein from *Macrobrachium rosenbergii* involved in *Spiroplasma eriocheiris* infection. Fish Shellfish Immunol 70:583–592

Qin Z, Sarath Babu V, Lin H, Dai Y, Kou H, Chen L, Li J, Zhao L, Lin L (2019) The immune function of prophenoloxidase from red swamp crayfish (*Procambarus clarkii*) in response to bacterial infection. Fish Shellfish Immunol 92:83–90

Sazer S (1996) The search for the primary function of the Ran GTPase continues. Trends Cell Biol 6:81–85

Seki T, Yamashita K, Nishitani H, Takagi T, Russell P, Nishimoto T (1992) Chromosome condensation caused by loss of RCC1 function requires the cdc25C protein that is located in the cytoplasm. Mol Biol Cell 3:1373–1388

Sun J, Zhao XL, Pei C, Zhu L, Zhang J, Kong XH (2022) Molecular characterization of NLRC3 and its interaction with other inflammasome components and regulation on the bacterial colonization in Qihe crucian carp *Carassius auratus*. Fish Shellfsh Immunol 131:958–971

Thabet R, Ayadi H, Koken M, Leignel V (2017) Homeostatic responses of crustaceans to salinity changes. Hydrobiologia 799:1–20

Toma-Fukai S, Shimizu T (2019) Structural insights into the regulation mechanism of small GTPases by GEFs. Molecules 24:3308

Wan H, Mu S, Baohua D, Guo S, Kang X (2022) Genome-wide investigation of toll-like receptor genes (TLRs) in *Procambarus clarkii* and their expression pattern in response to black may disease. Fish Shellfish Immunol 131(775):784

Wang Y, Lu Y, Zhang Y, Ning Z, Li Y, Zhao Q, Lu H, Huang R, Xia X, Feng Q, Liang X, Liu K, Zhang L, Lu T, Huang T, Fan D, Weng Q, Zhu C, Lu Y, Li W, Wen Z, Zhou C et al (2015) The draft genome of the grass carp (*Ctenopharyngodon idellus*) provides insights into its evolution and vegetarian adaptation. Nat Genet 47:625–631

Wang T, Jin S, Lv R, Meng Y, Li G, Han Y, Zhang Q (2023) Development of an indirect ELISA for detection of the adaptive immune response of black carp (*Mylopharyngodon piceus*). J Immunol Methods 521:113550

Wu W, Zong R, Xu J, Zhang X (2008) Antiviral phagocytosis is regulated by a novel Rab-dependent complex in shrimp *Penaeus japonicus*. J Proteome Res 7:424–431

Yang Z (2002) Small GTPases: versatile signaling switches in plants. Plant Cell 14:S375–S388

Zhao Y, Zhang J, Qiao D, Gao F, Gu Y, Jiang X, Zhu L, Kong X (2023a) CcGSDMEa functions the pore-formation in cytomembrane and the regulation on the secretion of IL-lβ in common carp (*Cyprinus carpio haematopterus*). Front Immunol 13:1110322

Zhao Y, Zhang J, Qiao D, Gao F, Jiang X, Zhao X, Hou L, Li H, Li L, Kong X (2023b) Functional roles of CcGSDMEa-like in common carp (*Cyprinus carpio*) after Aeromonas hydrophila infection. Fish Shellfish Immunol 142:109103

Zhou F, Zheng L, Yang Q, Qiu L, Huang J, Su T, Jiang S (2012) Molecular analysis of a ras-like nuclear (Ran) gene from *Penaeus monodon* and its expression at the different ovarian stages of development. Mol Biol Rep 39:3821–3827

Zhu L, Yuan G, Wang X, Zhao T, Hou L, Li C, Jiang X, Zhang J, Zhao X, Pei C, Li L, Kong X (2022) Molecular characterization of Rab7 and its involvement in innate immunity in red swamp crayfish *Procambarus clarkii*. Fish Shellfish Immunol 127:318–328